Hyperfine Interact (2006) 170:91–104
DOI 10.1007/s10751-006-9467-2

A complete solution to the Mössbauer problem, all in one place

C. J. Voyer · D. H. Ryan

Published online: 21 December 2006

Abstract We present a full solution to the general combined interactions static Mössbauer problem that is easily generalized to any Mössbauer isotope, and applies for M1, E1, and E2 transitions as well as combined M1–E2 transitions. Explicit expressions are given for both powder and single crystal samples.

Key words Mössbauer spectrum calculation · full Hamiltonian diagonalization · combined hyperfine interactions

1 Introduction

While first-order perturbation approaches or interpolation schemes are adequate for fitting the majority of simple Mössbauer spectra, there are numerous cases for which these approaches are invalid. If contributions from magnetic and electrostatic interactions are of comparable magnitude or do not share a common quantization axis, a full solution to the nuclear Hamiltonian must be used to fit the spectrum.

Although functional codes have been published in the past [1–3], in the current computational climate, where not only programming languages compete, but where computional packages that include programmable options (Matlab, Mathematica...) are also used, an explicit and adaptable mathematical solution is more useful. Most calculations given are either not worked out completely [1, 3], or are far too involved mathematically to be easily generalized and implemented into simple programs [4].

In order to promote the more widespread implementation of full solution Mössbauer fitting codes, we present here a complete solution that we have developed. This solution can be generalized to cover any accessible Mössbauer isotope and is cast in a form that can be readily coded into a fitting routine.

C. J. Voyer · D. H. Ryan (✉)
Centre for the Physics of Materials and Physics Department, McGill University,
3600 University Street, Montréal, QC H3A 2T8, Canada
e-mail: dominic@physics.mcgill.ca

2 The Mössbauer problem

The Mössbauer problem consists of computing a Mössbauer spectrum given a set of hyperfine parameters. The solution can then be used in a least squares refinement of an experimentally obtained Mössbauer spectrum. The line positions depend on the splitting of the ground and excited states and their relative energy difference, and can be derived from the eigenvalues of the system Hamiltonian. Line intensities depend on the coupling of the two angular momentum states involved in the transition, and can be obtained from the eigenvectors of the Hamiltonian combined with appropriate vector coupling coefficients [5]. In the absence of hyperfine fields, the ground and excited states are degenerate, and a single line spectrum is observed. When an electric field gradient, or a magnetic field, or both are present, the degeneracy is lifted and multi-line spectra are obtained as shown in Figure 1.

In the static model, the interaction Hamiltonian $\mathcal{H}$ is given by [6]:

$$\mathcal{H} = \mathcal{H}_\circ + \mathcal{H}_C + \mathcal{H}_M + \mathcal{H}_Q + \ldots \tag{1}$$

$\mathcal{H}_\circ$ represents all terms for the atom not including hyperfine interactions and does not influence the energy difference between the ground and excited states of the nucleus. Having no impact on the Mössbauer spectrum, it is ignored. $\mathcal{H}_C$ represents the Coulombic interactions between the nucleus and the electrons, i.e. the electric monopole term, and has the effect of shifting all excited state energy levels with respect to all ground state energy levels, and is called the isomer shift (IS). The IS will have the effect of shifting the entire Mössbauer spectrum either up or down in velocity. Other effects can also shift the entire spectrum by some constant velocity value, and so for fitting purposes we consider the more general centre shift (CS), which can be added to any solution once the more complex calculations are completed. Finally, $\mathcal{H}_M$ and $\mathcal{H}_Q$, the magnetic dipole and electric quadrupole contributions, are the terms that lift the energy level degeneracy, and are the non-trivial part of the computation. All higher order terms are ignored [6].

2.1 Magnetic dipole interactions

For a nucleus in a state with a gyromagnetic ratio g, and subject to a hyperfine magnetic field $\mathbf{B}$, $\mathcal{H}_M$ can written as [7]:

$$\mathcal{H}_M = -g\mu_N \mathbf{B} \cdot \hat{\mathbf{I}} \tag{2}$$

where $\hat{\mathbf{I}}$ is the total spin operator and μ_N is the nuclear magneton. For simplicity, we may choose the z-axis to be the direction of the field and get:

$$\mathcal{H}_M = -g\mu_N B \hat{I}_z \tag{3}$$

where B is the magnitude of the field and $\hat{I}_z$ is the z component of the angular momentum operator. For both the excited and ground states, the $|m\rangle$ states are eigenstates of this Hamiltonian and thus the eigenvalues are:

$$E_M = -g\mu_N Bm \tag{4}$$

and the eigenvector matrix is simply identity.

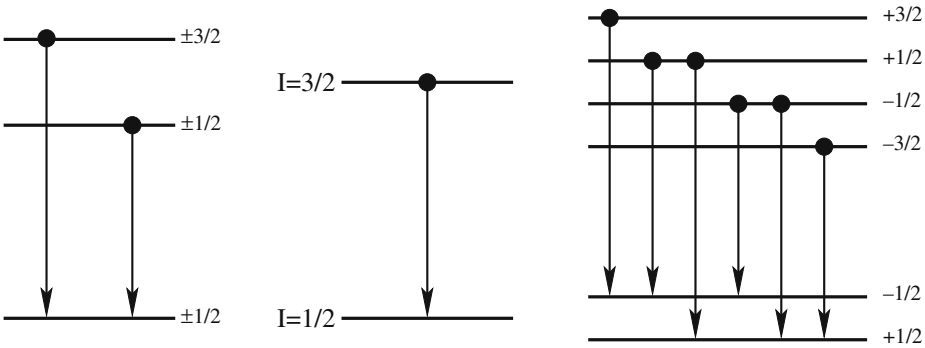

Figure 1 Sketch of energy level degeneracy lifting in the ^{57}Fe case. In the *centre* we see the degenerate excited and ground states, on the *left* the excited state has the degeneracy partially lifted when an electric field gradient is present, and on the *right* when a magnetic field is present, we see the degeneracy completely lifted. The *arrows drawn* are the allowed transitions given the M1 multipolarity.

2.2 Electric quadrupole interactions

The nuclear energy level degeneracy is also lifted by the quadrupole moment of the probe nucleus interacting with an electric field gradient. The electric field gradient is a 3×3 traceless tensor:

$$V_{ij} = (\partial^2 V/\partial x_i \partial x_j) \qquad (x_i, x_j = x, y, z). \tag{5}$$

The coordinate system can always be chosen such that the tensor is diagonal and traditionally the z-axis is chosen so that V_{zz} is its largest component. Since the tensor is traceless, $V_{xx} + V_{yy} + V_{zz} = 0$, only two parameters are required to specify the tensor completely. We define $\eta = \frac{V_{xx} - V_{yy}}{V_{zz}}$, using the convention $|V_{zz}| \geq |V_{yy}| \geq |V_{xx}|$ to ensure that $0 \leq \eta \leq 1$, and the tensor can be specified by V_{zz} and η . For a nucleus with an electric quadrupole moment Q, spin I, subject to an electric field gradient whose principal axis value is V_{zz}, with an asymmetry η, the Hamiltonian is [8]:

$$\mathcal{H}_Q = \frac{eQV_{zz}}{4I(2I-1)}\left[3\hat{I}_z^2 - I(I+1) + \frac{\eta}{2}(\hat{I}_+^2 - \hat{I}_-^2)\right] \tag{6}$$

where e is the charge of the proton and $\hat{I}_+$ and $\hat{I}_-$ are the ladder operators as defined by Sakurai [9].

If $\eta = 0$ the $|m\rangle$ states are energy eigenstates and the energies are $E_m = \frac{eQV_{zz}}{4I(2I-1)}\left[3m^2 - I(I+1)\right]$, which in turn yields a degeneracy in the energy levels as only the magnitude of m contributes to the energy. Complications arise when $\eta \neq 0$ since in this case the $|m\rangle$ states are no longer energy eigenstates. The Hamiltonian is then non-diagonal and the eigenvectors need to be computed explicitly and a full diagonalization is necessary.

A fitting routine needs to compute a full spectrum many times in order to complete a pattern refinement. Available computing power used to limit solution possibilities, and strategies were devised to avoid repeated calculation of the full solution. Exact analytic solutions for the energy levels exist for the $I = \frac{3}{2}$ case [10], and the $I = \frac{5}{2}$ case

[11], however, when the dimensions of the Hamiltonian get larger the mathematics of an analytic solution becomes prohibitively difficult. Shenoy et al. [12] generated a polynomial interpolation scheme, where the line positions and intensities have been computed exactly for incremental values of η and then fit with a polynomial whose coefficients were made available. Finally the perturbative approach is useful if one of the interactions is small compared to the other. Today, however, computing power limitations for this type of calculation no longer exist, and the only remaining barrier to a full solution is the mathematics involved.

The ideal situation is to have a solution to the Mössbauer problem that can be implemented easily as a numerical routine that yields exact line positions and intensities given a set of hyperfine parameters, with no limitations on the values of these parameters. This solution could then be incorporated into a least squares fitting routine and refine experimentally obtained data. Numerical diagonalization is longer a limitation. We can solve the general static Mössbauer problem exactly, and have a solution that can cover the most complex cases, as well as covering simple cases, that can be easily implemented, operate efficiently and satisfy all fitting needs.

3 Combined interactions

The most general physical situation that can be considered is the case of combined magnetic dipole and electric quadrupole interactions. In the previous cases considered, the optimal choice of quantization axis was evident. Here we have two logical choices: the magnetic field direction, or the principal axis of the electric field gradient, V_{zz}. Typically, V_{zz} is chosen as the quantization axis and the schematic setup is shown in Figure 2. Note that this choice of axes is valid even if $V_{zz} = 0$, and none of the computations change.

From (1), the Hamiltonian operator for this system becomes [8]:

$$\mathcal{H} = \mathcal{H}_Q + \mathcal{H}_M \tag{7}$$

where $\mathcal{H}_Q$ does not change from (6), but $\mathcal{H}_M$ needs to be rotated away from the z-axis and can be written following the convention of Figure 2 as:

$$\mathcal{H}_M = -g\mu_N B_{hf}\left[\hat{I}_z \cos\theta + \frac{1}{2}(\hat{I}_+ e^{-i\phi} + \hat{I}_- e^{i\phi}) \sin\theta\right] \tag{8}$$

This Hamiltonian will not, in general, be diagonal in the $|m\rangle$ basis.

To compute the energy eigenvalues and eigenvectors we need to write the Hamiltonian in matrix form. The expression for the matrix depends on the total spins I_g and I_e of the ground and excited states. Once the Mössbauer transition is chosen, and I_g and I_e are thereby fixed, we can write the Hamiltonian for the ground and excited states, $\mathcal{H}_g$ and $\mathcal{H}_e$.

For example, if we are interested in a $\frac{3}{2} \rightarrow \frac{1}{2}$ transition (as in ^{57}Fe, ^{119}Sn …) or a $\frac{1}{2} \rightarrow \frac{3}{2}$ (as in ^{189}Os, ^{197}Au…) transition, if we set $A = \frac{eQV_{zz}}{4I(2I-1)}$ where Q is the appropriate value for the quadrupole moment of the nucleus in the $I = \frac{3}{2}$ state, and

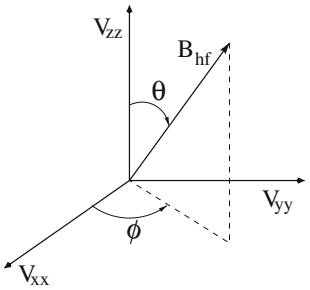

Figure 2 Schematic of the ϕ and θ angles, V_{zz} and B_{hf} as they appear in the Hamiltonian of (7).

$\alpha = g_{\frac{3}{2}}\mu_N B_{hf}$, where $g_{\frac{3}{2}}$ is the appropriate value for the gyromagnetic factor of the nucleus in the $I = \frac{3}{2}$ state, we may write (matrices constructed as described in [13]):

$$\mathcal{H}_{3/2} = \begin{pmatrix} 3A - \frac{3}{2}\alpha\cos\theta & -\frac{\sqrt{3}}{2}\alpha\sin\theta e^{-i\phi} & \sqrt{3}A\eta & 0 \\ -\frac{\sqrt{3}}{2}\alpha\sin\theta e^{i\phi} & -3A - \frac{\alpha}{2}\cos\theta & -\alpha\sin\theta e^{-i\phi} & \sqrt{3}A\eta \\ \sqrt{3}A\eta & -\alpha\sin\theta e^{i\phi} & -3A + \frac{\alpha}{2}\cos\theta & -\frac{\sqrt{3}}{2}\alpha\sin\theta e^{-i\phi} \\ 0 & \sqrt{3}A\eta & -\frac{\sqrt{3}}{2}\alpha\sin\theta e^{i\phi} & 3A + \frac{3}{2}\alpha\cos\theta \end{pmatrix} \tag{9}$$

and setting $\beta = g_{1/2}\mu_N B_{hf}$:

$$\mathcal{H}_{1/2} = \begin{pmatrix} -\frac{\beta}{2}\cos\theta & -\frac{\beta}{2}\sin\theta e^{-i\phi} \\ -\frac{\beta}{2}\sin\theta e^{+i\phi} & +\frac{\beta}{2}\cos\theta \end{pmatrix} \tag{10}$$

The $I = 0$ case is of particular mathematical interest because the Hamiltonian in (7) is null. This case is treated by considering the state to have a unidimensional eigenvector in the $|m\rangle$ basis, and an energy eigenvalue of 0. So if we are interested in the $2 \to 0$ transition (^{170}Yb, ^{166}Er…), the only Hamiltonian that needs to be explicitly computed is the $I = 2$ excited state Hamiltonian (here $\beta = g_2\mu_N B_{hf}$):

$$\mathcal{H}_2 = \begin{pmatrix} 6A - 2\beta\cos\theta & -\beta e^{-i\phi}\sin\theta & A\sqrt{6}\eta & 0 & 0 \\ -\beta e^{i\phi}\sin\theta & -3A - \beta\cos\theta & -\frac{\sqrt{6}}{2}\beta\sin\theta e^{-i\phi} & 3A\eta & 0 \\ A\sqrt{6}\eta & -\beta\frac{\sqrt{6}}{2}e^{i\phi}\sin\theta & -6A & -\frac{\sqrt{6}}{2}\beta\sin\theta e^{-i\phi} & B\sqrt{6}\eta \\ 0 & 3A\eta & -\frac{\sqrt{6}}{2}\beta\sin\theta e^{i\phi} & -3A + \beta\cos\theta & -\beta\sin\theta e^{-i\phi} \\ 0 & 0 & A\sqrt{6}\eta & -\beta\sin\theta e^{i\phi} & 6A + 2\beta\cos\theta \end{pmatrix} \tag{11}$$

With the excited and ground state Hamiltonians now analytically expressed, a routine may compute the components, given a set of hyperfine parameters, then proceed to the numerical diagonalization, and finally compute the line positions and intensities.

Many options are available for the numerical diagonalization. We have used the `tred2` and `tqli` routines outlined in Numerical Recipes [14, 15]. The Matlab and Mathematica software packages also offer diagonalization functions. To avoid working with complex numbers Numerical Recipes suggests a scheme by which the matrix can be kept real, however it requires doubling the dimensionality of the problem. After diagonalization is achieved, the problem is then reduced back to its original dimension by selecting half of the eigenvalues and eigenvectors. The selection must be done with care since the ordering of the diagonalization output depends on the set of non-zero hyperfine parameters. The selection must ensure a set of mutually orthogonal eigenvectors is obtained.

From these routines, we obtain numerical values for our eigenvectors $|e_n\rangle$ as well as the amplitudes $\langle n|m\rangle$ and the eigenvalues of the system. For a state with total spin I and corresponding eigenvalues e_n, for example:

$$|e_n\rangle = \begin{pmatrix} \langle m = I|n_{e_n}\rangle \\ \langle m = I-1|n_{e_n}\rangle \\ \langle m = I-2|n_{e_n}\rangle \\ \vdots \end{pmatrix} \tag{12}$$

At this stage we have the eigenvalues which will give us the line positions, and the $\langle m|n\rangle$ factors which will give us the intensity of each line. We have thus obtained all the necessary information from the Hamiltonians of the excited and ground states, and may now proceed to calculate the exact line positions and intensities.

3.1 Line position calculation

The energy shift detected by Mössbauer spectroscopy is the difference between the energies of the excited state Hamiltonian E_{n_e} and the ground state Hamiltonian E_{n_g}. For a given transition between the levels E_{n_g} of the ground state and E_{n_e} of the excited state, we obtain a line position $E_n(e \to g)$:

$$E_n(e \to g) = E_{n_e} - E_{n_g} \tag{13}$$

The constant offset CS mentioned in Section 2 can then be added, and the final result is completely general for all values of the hyperfine parameters. We note that for the specific case of the $2 \to 0$ transition (^{170}Yb), this reduces to:

$$E_n(2 \to 0) = E_{n_2} + CS \tag{14}$$

The number of lines observed will depend on the dimensionality of both $\mathcal{H}_e$ and $\mathcal{H}_g$, and also on the multipolarity of the transition i.e. the quantum mechanical selection rules that apply in each situation.

3.2 Line intensity calculation

The relative probability of each transition's occurrence will depend on the coupling of the two angular momentum states involved in the transition [5]. Several methods exist for calculating the relative intensity of a line [3, 5, 8, 16]. These treatments fall short however, in that they either treat a single case [8], do not treat the E2 case [16],

do not give an explicit and easily generalizable solution [3, 5, 8, 16], or do not cover the single crystal case [3, 5, 8].

We chose to treat the relative intensity of a line in a spectrum as the normalized power absorbed by the corresponding transition. We write the multipole electric field vector **E** as [17]:

$$\mathbf{E}(\varphi, \vartheta) = \sum_{l,m} (-i)^{l+1} \left[a_E(l,m)\mathbf{X}_l^m \times \mathbf{r} + a_M(l,m)\mathbf{X}_l^m \right] \tag{15}$$

where ϑ and φ are the polar angles describing the direction of emission of the γ, along **r**, with respect to our chosen axis of quantization (not to be confused with ϕ and θ defined in Section 3); $\mathbf{X}_l^m$ are the vector spherical harmonics, and will be derived later (Section 3.3); and the $a_E(l,m)$ and $a_M(l,m)$ specify the amounts of electric multipole and magnetic multipole fields, and are determined by the source and by boundary conditions (derived in Section 3.4) [18].

Since we are only concerned with relative intensities, factors common to all transitions can be normalized out and so are omitted from (15). The power absorbed (i.e. the intensity of a line) will be $\mathbf{E}.\mathbf{E}^*$. This method simply and naturally introduces the vector spherical harmonics needed, and leads to a straightforward single crystal intensity as well as a powder average intensity. This method is preferred because of its simple computations and adaptability to different transitions the experimentalist may face.

The three transition multipolarities encountered in Mössbauer spectroscopy are the M1, E1 and E2 cases. Only the M1 and E2 are ever combined, and the E1 case is completely analogous to the M1 case and requires no new information, thus for the purposes of this computation, we will not address the E1 case.

From (15) we get for the M1 case,

$$\mathbf{E}_{M1}(\varphi, \vartheta) = -\sum_{m=-1}^{+1} a_M(1,m).\mathbf{X}_l^m \tag{16}$$

and for the E2 case we get

$$\mathbf{E}_{E2}(\varphi, \vartheta) = \sum_{m=-2}^{+2} i.\left[a_E(2,m)\right].(\mathbf{X}_l^m \times \mathbf{r}) \tag{17}$$

To proceed further, we need to express **E** more explicitly, thus calculating the vector spherical harmonics $\mathbf{X}_l^m$, and the amounts of electric and magnetic multipole fields $a_E(l,m)$ and $a_M(l,m)$.

3.3 The $\mathbf{X}_l^m$

The vector spherical harmonics, $\mathbf{X}_l^m$, can be generated from [18]

$$\mathbf{X}_l^m = \frac{1}{\sqrt{l(l+1)}} \hat{\mathbf{L}} Y_l^m(\vartheta, \varphi) \tag{18}$$

where,

$$\hat{\mathbf{L}} = i\left(\hat{\vartheta}\frac{1}{\sin\vartheta}\frac{\partial}{\partial\varphi} - \hat{\varphi}\frac{\partial}{\partial\vartheta}\right) \tag{19}$$

We compute the vector spherical harmonics needed,

$$\mathbf{X}_1^{-1} = \frac{1}{4}\sqrt{\frac{3}{\pi}}\left(e^{-i\varphi}\hat{\vartheta} - i\cos\vartheta e^{-i\varphi}\hat{\varphi}\right) \tag{20}$$

$$\mathbf{X}_1^{0} = \frac{1}{4}\sqrt{\frac{3}{\pi}}i\sqrt{2}\sin\vartheta\hat{\varphi} \tag{21}$$

$$\mathbf{X}_1^{1} = \frac{1}{4}\sqrt{\frac{3}{\pi}}\left(e^{i\varphi}\hat{\vartheta} + i\cos\vartheta e^{i\varphi}\hat{\varphi}\right) \tag{22}$$

$$\mathbf{X}_2^{-2} = \frac{1}{4}\sqrt{\frac{5}{\pi}}\left(\sin\vartheta e^{-2i\varphi}\hat{\vartheta} - i\sin\vartheta\cos\vartheta e^{-2i\varphi}\hat{\varphi}\right) \tag{23}$$

$$\mathbf{X}_2^{-1} = \frac{1}{4}\sqrt{\frac{5}{\pi}}\left(\cos\vartheta e^{-i\varphi}\hat{\vartheta} - i\left[\cos^2\vartheta - \sin^2\vartheta\right]e^{-i\varphi}\hat{\varphi}\right) \tag{24}$$

$$\mathbf{X}_2^{0} = \frac{1}{4}\sqrt{\frac{5}{\pi}}\left(\sqrt{6}i\cos\vartheta\sin\vartheta\right)\hat{\varphi} \tag{25}$$

$$\mathbf{X}_2^{1} = \frac{1}{4}\sqrt{\frac{5}{\pi}}\left(\cos\vartheta e^{i\varphi}\hat{\vartheta} + i\left[\cos^2\vartheta - \sin^2\vartheta\right]e^{i\varphi}\hat{\varphi}\right) \tag{26}$$

$$\mathbf{X}_2^{2} = \frac{1}{4}\sqrt{\frac{5}{\pi}}\left(-\sin\vartheta e^{2i\varphi}\hat{\vartheta} - i\sin\vartheta\cos\vartheta e^{2i\varphi}\hat{\varphi}\right) \tag{27}$$

We note that in spherical coordinates $\hat{\vartheta}\times\hat{r} = \hat{\varphi}$ and that $\hat{\varphi}\times\hat{r} = -\hat{\vartheta}$, such that for the $\mathbf{X}_2^m$ of the E2 part we get

$$\mathbf{X}_2^{-2}\times\hat{r} = \frac{1}{4}\sqrt{\frac{5}{\pi}}\left(\sin\vartheta e^{-2i\varphi}\hat{\varphi} + i\sin\vartheta\cos\vartheta e^{-2i\varphi}\hat{\vartheta}\right) \tag{28}$$

$$\mathbf{X}_2^{-1}\times\hat{r} = \frac{1}{4}\sqrt{\frac{5}{\pi}}\left(\cos\vartheta e^{-i\varphi}\hat{\varphi} + i\left[\cos^2\vartheta - \sin^2\vartheta\right]e^{-i\varphi}\hat{\vartheta}\right) \tag{29}$$

$$\mathbf{X}_2^{0}\times\hat{r} = \frac{1}{4}\sqrt{\frac{5}{\pi}}\left(-\sqrt{6}i\cos\vartheta\sin\vartheta\right)\hat{\vartheta} \tag{30}$$

$$\mathbf{X}_2^{1}\times\hat{r} = \frac{1}{4}\sqrt{\frac{5}{\pi}}\left(\cos\vartheta e^{i\varphi}\hat{\varphi} - i\left[\cos^2\vartheta - \sin^2\vartheta\right]e^{i\varphi}\hat{\vartheta}\right) \tag{31}$$

$$\mathbf{X}_2^{2}\times\hat{r} = \frac{1}{4}\sqrt{\frac{5}{\pi}}\left(-\sin\vartheta e^{2i\varphi}\hat{\varphi} + i\sin\vartheta\cos\vartheta e^{2i\varphi}\hat{\vartheta}\right) \tag{32}$$

3.4 The $a(\mathbf{L}, m)$

For this particular problem, the $a_E(\mathbf{L}, m)$ and $a_M(\mathbf{L}, m)$ coefficients have the same analytic expression [16],

$$a(\mathbf{L}, m) = \sum_{m_e - m_g = m} \langle m_e|n_e\rangle \langle m_g|n_g\rangle^* \langle I_g \mathbf{L} m_g m | I_e m_e\rangle \tag{33}$$

where $|n_g\rangle$ and $|n_e\rangle$ are the energy eigenstates of the ground and excited states respectively, and $|m_e\rangle$ and $|m_g\rangle$ are the $\hat{I}_z$ eigenstates for the excited and ground states respectively, (note that $\langle m_e|n_e\rangle$ and $\langle m_g|n_g\rangle$ are simply the components of the eigenvectors of $\mathcal{H}_e$ and $\mathcal{H}_g$, respectively), and $\langle I_g \mathbf{L} m_g m | I_e m_e\rangle$ are Clebsch-Gordan coefficients where $\mathbf{L}$ is the multipolarity of the transition (for M1, $\mathbf{L} = 1$ and for E2, $\mathbf{L} = 2$), $m = m_e - m_g$, I_e is the total spin of the excited state and I_g is the total spin of the ground state.

For the $2 \rightarrow 0$ transition, all Clebsch-Gordon coefficients are exactly 1 since $I_g = 0$. But if the spins for both the excited and ground states are non-zero, the Clebsch-Gordon coefficients are non-trivial (see Table I for an example). Note that the $\langle I_g \mathbf{L} m_g m | I_e m_e\rangle$ coefficients are first converted using the relation [19]:

$$\langle I_g \mathbf{L} m_g m | I_e m_e\rangle = (-1)^{I_g - m_g} \sqrt{\frac{2I_e + 1}{2(I_e - I_g) + 1}} \langle I_e I_g m_e - m_g | \mathbf{L} m\rangle \tag{34}$$

Once an expression for the Clebsch-Gordon coefficients is obtained we can move on to calculating the $a(\mathbf{L}, m)$ explicitly. Again, for the case of a $3/2 \rightarrow 1/2$ transition we get,

$$a(2, 2) = -\sqrt{\frac{4}{5}} \langle 3/2|n_e\rangle \langle -1/2|n_g\rangle^*$$

$$a(2, 1) = \sqrt{\frac{1}{5}} \langle 3/2|n_e\rangle \langle 1/2|n_g\rangle^* - \sqrt{\frac{3}{5}} \langle 1/2|n_e\rangle \langle -1/2|n_g\rangle^*$$

$$a(2, 0) = \sqrt{\frac{2}{5}} \langle 1/2|n_e\rangle \langle 1/2|n_g\rangle^* - \sqrt{\frac{2}{5}} \langle -1/2|n_e\rangle \langle -1/2|n_g\rangle^*$$

$$a(2, -1) = \sqrt{\frac{3}{5}} \langle -1/2|n_e\rangle \langle 1/2|n_g\rangle^* - \sqrt{\frac{1}{5}} \langle -3/2|n_e\rangle \langle -1/2|n_g\rangle^*$$

$$a(2, -2) = \sqrt{\frac{4}{5}} \langle -3/2|n_e\rangle \langle 1/2|n_g\rangle^*$$

$$a(1, 1) = \sqrt{\frac{1}{3}} \langle 1/2|n_e\rangle \langle -1/2|n_g\rangle^* + \langle 3/2|n_e\rangle \langle 1/2|n_g\rangle^*$$

$$a(1, 0) = \sqrt{\frac{2}{3}} \langle 1/2|n_e\rangle \langle 1/2|n_g\rangle^* + \sqrt{\frac{2}{3}} \langle -1/2|n_e\rangle \langle -1/2|n_g\rangle^*$$

$$a(1, -1) = \sqrt{\frac{1}{3}} \langle -1/2|n_e\rangle \langle 1/2|n_g\rangle^* + \langle -3/2|n_e\rangle \langle -1/2|n_g\rangle^*$$

Table I Clebsch-Gordon coefficients pertinent to the $3/2 \rightarrow 1/2$ M1 and/or E2 solution

m_g	m_e	m	E2 $\langle \frac{1}{2}\mathbf{2}m_g m \vert \frac{3}{2}m_e\rangle$	M1 $\langle \frac{1}{2}\mathbf{1}m_g m \vert \frac{3}{2}m_e\rangle$
$+\frac{1}{2}$	$+\frac{3}{2}$	$+1$	$\sqrt{\frac{1}{5}}$	1
$+\frac{1}{2}$	$+\frac{1}{2}$	0	$\sqrt{\frac{2}{5}}$	$\sqrt{\frac{2}{3}}$
$+\frac{1}{2}$	$-\frac{1}{2}$	-1	$\sqrt{\frac{3}{5}}$	$\sqrt{\frac{1}{3}}$
$+\frac{1}{2}$	$-\frac{3}{2}$	-2	$\sqrt{\frac{4}{5}}$	0
$-\frac{1}{2}$	$+\frac{3}{2}$	$+2$	$-\sqrt{\frac{4}{5}}$	0
$-\frac{1}{2}$	$+\frac{1}{2}$	$+1$	$-\sqrt{\frac{3}{5}}$	$\sqrt{\frac{1}{3}}$
$-\frac{1}{2}$	$-\frac{1}{2}$	0	$-\sqrt{\frac{2}{5}}$	$\sqrt{\frac{2}{3}}$
$-\frac{1}{2}$	$-\frac{3}{2}$	-1	$-\sqrt{\frac{1}{5}}$	1

where the $a(2, m)$ are for the E2 multipolarity case, and the $a(1, m)$ are for the M1 multipolarity case. For the $2 \rightarrow 0$ case with E2 multipolarity however, the expressions become much simpler,

$$
\begin{aligned}
a(2, 2) &= \langle 2|n_e\rangle \\
a(2, 1) &= \langle 1|n_e\rangle \\
a(2, 0) &= \langle 0|n_e\rangle \\
a(2, -1) &= \langle -1|n_e\rangle \\
a(2, -2) &= \langle -2|n_e\rangle
\end{aligned}
$$

The vectors in (16) and (17) now have numerical values. We can now move on to calculating the intensity of each line.

3.5 M1 transitions

We first consider the case of an M1 transition (^{57}Fe, ^{119}Sn…). The electric field vector can be written as:

$$
\begin{aligned}
\mathbf{E}_{M1}(\varphi, \vartheta) = \frac{1}{4}\sqrt{\frac{5}{\pi}}\sqrt{\frac{3}{5}}\Bigg(&\Big[a(1, 1)e^{i\varphi} + a(1, -1)e^{-i\varphi}\Big]\hat{\vartheta} \\
&+ i\Big[a(1, 1)e^{i\varphi}\cos\vartheta + a(1, 0)\sqrt{2}\sin\vartheta - a(1, -1)e^{-i\varphi}\cos\vartheta\Big]\hat{\varphi}\Bigg)
\end{aligned}
\tag{35}
$$

Noting that $\hat{\varphi}.\hat{\vartheta} = 0$, the intensity of a line can be written as:

$$\begin{aligned}\mathbf{E}_{M1}.\mathbf{E}^*_{M1} = \frac{3}{16\pi}\Big(&|a(1,1)|^2(1+\cos^2\vartheta) + 2|a(1,0)|^2\sin^2\vartheta \\ &+ |a(1,-1)|^2(1+\cos^2\vartheta) + 2\Re\left[a(1,1)a^*(1,-1)e^{2i\varphi}\right] \\ &+ 2\Re\left[a(1,1)a^*(1,0)\sqrt{2}\sin\vartheta\cos\vartheta e^{i\varphi}\right] \\ &- 2\Re\left[a(1,1)a^*(1,-1)\cos^2\vartheta e^{2i\varphi}\right] \\ &- 2\Re\left[a(1,0)a^*(1,-1)\sqrt{2}\sin\vartheta\cos\vartheta e^{i\varphi}\right]\Big)\end{aligned} \tag{36}$$

Equation 36 is the intensity for a line in a single crystal Mössbauer absorption with a γ absorption that makes angles φ and ϑ with respect to the principal axis of the electric field gradient V_{zz}. The $\frac{3}{16\pi}$ factor can be ignored as it is the same for all transitions.

Most samples used are polycrystalline, in which the intensity needs to be integrated over all directions. The intensity for a powder sample becomes:

$$\int_{\vartheta=0}^{\pi}\int_{\varphi=0}^{2\pi}\mathbf{E}_{M1}.\mathbf{E}^*_{M1}\sin\vartheta\,\mathrm{d}\varphi\mathrm{d}\vartheta = |a(1,1)|^2 + |a(1,0)|^2 + |a(1,-1)|^2 \tag{37}$$

We note that although one of the most cited solutions of the Mössbauer problem (Kündig's solution of the ^{57}Fe problem [8]) yields a slightly different expression, his expression can be simplified to obtain (37), providing an independent verification that our process is correct.

3.6 E2 transitions

For an E2 transition the selection rules are less restrictive and far more transitions are allowed. The electric field vector can be written as:

$$\begin{aligned}\mathbf{E}_{E2} = \frac{1}{4}\sqrt{\frac{5}{\pi}}\Big(\Big[&-a(2,-2)\sin\vartheta\cos\vartheta e^{-2i\varphi} - a(2,-1)\left[\cos^2\vartheta - \sin^2\vartheta\right]e^{-i\varphi} \\ &+ a(2,0)\sqrt{6}\cos\vartheta\sin\vartheta + a(2,1)\left[\cos^2\vartheta - \sin^2\vartheta\right]e^{i\varphi} \\ &- a(2,2)\sin\vartheta\cos\vartheta e^{2i\varphi}\Big]\hat{\vartheta} + i\Big[a(2,-2)\sin\vartheta e^{-2i\varphi} \\ &+ a(2,-1)\cos\vartheta e^{-i\varphi} + a(2,1)\cos\vartheta e^{i\varphi} - a(2,2)\sin\vartheta e^{2i\varphi}\Big]\hat{\varphi}\Big)\end{aligned} \tag{38}$$

The intensity is then:

$$
\begin{aligned}
\mathbf{E}_{E2}.\mathbf{E}^*_{E2} = \frac{5}{16\pi}\Big(& |a(2,-2)|^2 \sin^2\vartheta(1+\cos^2\vartheta) + |a(2,-1)|^2\left(\left[\cos^2\vartheta - \sin^2\vartheta\right]^2 + \cos^2\vartheta\right) \\
& + 6|a(2,0)|^2\cos^2\vartheta\sin^2\vartheta + |a(2,1)|^2\left(\left[\cos^2\vartheta - \sin^2\vartheta\right]^2 + \cos^2\vartheta\right) \\
& + |a(2,2)|^2\left(\sin^2\vartheta\cos^2\vartheta + \sin^2\vartheta\right) \\
& + 2\Re\left\{a(2,-2)a^*(2,-1)\sin\vartheta\cos\vartheta\left[\cos^2\vartheta - \sin^2\vartheta\right]e^{-i\varphi}\right\} \\
& - 2\Re\left\{a(2,-2)a^*(2,0)\sqrt{6}\cos^2\vartheta\sin^2\vartheta e^{-2i\varphi}\right\} \\
& - 2\Re\left\{a(2,-2)a^*(2,1)\sin\vartheta\cos\vartheta\left[\cos^2\vartheta - \sin^2\vartheta\right]e^{-3i\varphi}\right\} \\
& + 2\Re\left\{a(2,-2)a^*(2,2)\cos^2\vartheta\sin^2\vartheta e^{-4i\varphi}\right\} \\
& - 2\Re\left\{a(2,-1)a^*(2,0)\sqrt{6}\sin\vartheta\cos\vartheta\left[\cos^2\vartheta - \sin^2\vartheta\right]e^{-i\varphi}\right\} \\
& - 2\Re\left\{a(2,-1)a^*(2,1)\left[\cos^2\vartheta - \sin^2\vartheta\right]^2 e^{-2i\varphi}\right\} \\
& + 2\Re\left\{a(2,-1)a^*(2,2)\sin\vartheta\cos\vartheta\left[\cos^2\vartheta - \sin^2\vartheta\right]e^{-3i\varphi}\right\} \\
& + 2\Re\left\{a(2,0)a^*(2,1)\sqrt{6}\sin\vartheta\cos\vartheta\left[\cos^2\vartheta - \sin^2\vartheta\right]e^{-i\varphi}\right\} \\
& - 2\Re\left\{a(2,0)a^*(2,2)\sqrt{6}\cos^2\vartheta\sin^2\vartheta e^{-2i\varphi}\right\} \\
& - 2\Re\left\{a(2,1)a^*(2,2)\sin\vartheta\cos\vartheta\left[\cos^2\vartheta - \sin^2\vartheta\right]e^{-i\varphi}\right\} \\
& + 2\Re\left[a(2,-2)a^*(2,-1)\cos\vartheta\sin\vartheta e^{-i\varphi}\right] \\
& + 2\Re\left[a(2,-2)a^*(2,1)\sin\vartheta\cos\vartheta e^{-3i\varphi}\right] \\
& - 2\Re\left[a(2,-2)a^*(2,2)\sin^2\vartheta e^{-4i\varphi}\right] \\
& + 2\Re\left[a(2,-1)a^*(2,1)\cos^2\vartheta e^{-2i\varphi}\right] \\
& - 2\Re\left[a(2,-1)a^*(2,2)\sin\vartheta\cos\vartheta e^{-3i\varphi}\right] \\
& - 2\Re\left[a(2,1)a^*(2,2)\cos\vartheta\sin\vartheta e^{-i\varphi}\right]\Big)
\end{aligned}
\tag{39}
$$

Again, as was done in Section 3.5, we integrate over all directions to obtain the intensities for the powder average case and obtain,

$$
\int_{\vartheta=0}^{\pi}\int_{\varphi=0}^{2\pi}\mathbf{E}.\mathbf{E}^*\sin\vartheta\,\mathrm{d}\vartheta\,\mathrm{d}\varphi = |a(2,-2)|^2 + |a(2,-1)|^2 + |a(2,0)|^2 + |a(2,1)|^2 + |a(2,2)|^2 \tag{40}
$$

a result which is analogous to the M1 case and completes the list of results necessary to compute the exact line intensity of any static combined interactions Mössbauer spectrum.

For the $2 \rightarrow 0$ case, the intensity expression is greatly simplified:

$$\begin{aligned}\int_{\vartheta=0}^{\pi}\int_{\varphi=0}^{2\pi}\mathbf{E}.\mathbf{E}^{*}\sin\vartheta\,\mathrm{d}\vartheta\,\mathrm{d}\varphi &= |\langle 2|i\rangle|^2 + |\langle 1|i\rangle|^2 + |\langle 0|i\rangle|^2 + |\langle -1|i\rangle|^2 + |\langle -2|i\rangle|^2 \\ &= \langle i|\left(\sum_m |m\rangle\,\langle m|\right)|i\rangle \\ &= 1 \end{aligned} \tag{41}$$

making the intensity computation unnecessary.

3.7 Mixed M1–E2 transitions

Certain Mössbauer isotopes have a mixture of M1 and E2 transitions in non-negligible amounts (e.g. ^{197}Au where E2/M1=0.11). If we define $\mathcal{X} = \frac{E2}{E2+M1}$, the intensity expression is:

$$\mathbf{E}.\mathbf{E}^{*} = (1-\mathcal{X})\,\mathbf{E}_{M1}.\mathbf{E}^{*}_{M1} + \mathcal{X}\mathbf{E}_{E2}.\mathbf{E}^{*}_{E2} \tag{42}$$

Thus the single crystal intensity for a combined E2-M1 transition is the weighted sum of (36) and (39), and the powder intensity is the weighted sum of (37) and (40).

4 Adapting the solution to other isotopes

When faced with an isotope not treated in the present text, the researcher may simply apply the same general strategy used here, and indeed the more complex expressions still hold. (36), (37), (39) and (40) do not change.

A new isotope brings new values for the total spin of the excited and ground states and different values for the quadrupole moments and gyromagnetic ratios for the excited and ground states. The spectra obtained from different isotopes will behave differently but the strategies outlined in this paper can be easily applied:

1. Set up the matrices $\mathcal{H}_e$ and $\mathcal{H}_g$, as was done in (9), (10) and (11).
2. Set up the chosen diagonalization routine and store proper set of eigenvalues and eigenvectors
3. Calculate the sum in (33) using the appropriate Clebsch-Gordon coefficients. The number of terms is set by: $m_e - m_g = m$, and the $\langle m|n\rangle$ are the components of the eigenvectors as shown in (12).
4. The intensities are computed using the relevant equation from (36),(37), (39), (40), or (42), depending on the transition multipolarity (M1,E2, or M1–E2) and whether the experiment is on a single crystal or powder sample.
5. The line positions are calculated using (13).

This strategy is completely general for any static combined interactions case, for any Mössbauer isotope.

References

1. Gabriel, J.R., Ruby, S.L.: Nucl. Instrum. Methods **36**, 23 (1965)
2. Kündig, W.: Nucl. Instrum. Methods **75**, 336 (1969)
3. Chipaux, R.: Comput. Phys. Commun. **60**, 405 (1990)
4. Szymański, K.: J. Phys., Condens. Matter **12**, 7495 (2000)
5. Gibb, T.C., Greenwood, N.N.: In: Mössbauer Spectroscopy, p.66. Chapman and Hall, London, UK (1971)
6. Gibb, T.C., Greenwood, N.N.: In: Mössbauer Spectroscopy, p.46. Chapman and Hall, London, UK (1971)
7. Gibb, T.C., Greenwood, N.N.: In: Mössbauer Spectroscopy, p.60. Chapman and Hall, London, UK (1971)
8. Kündig, W.: Nucl. Instrum. Methods **48**, 219 (1967)
9. Sakurai, J.J.: In: Modern Quantum Mechanics, 2nd edn., p.192. Addison-Wesley, New York (1994)
10. Gibb, T.C., Greenwood, N.N.: In: Mössbauer Spectroscopy, p.56. Chapman and Hall, London, UK (1971)
11. Gerdau, E., Wolf, J., Winkler, H., Braunsfurth, J.: Proc. Roy. Soc. Ser. A **311**, 197–206 (1969)
12. Shenoy, G.K., Dunlap, B.D.: Nucl. Instrum. Methods **71**, 285 (1969)
13. Sakurai, J.J.: In: Modern Quantum Mechanics, 2nd edn., p.20. Addison-Wesley, New York (1994)
14. Press, W.H., Tukolsky, S.A., Vetterling, W.T., Flannery, B.P.: In: Numerical Recipes in C, 2nd edn., p.474. Cambridge University Press, New York (1999)
15. Press, W.H., Tukolsky, S.A., Vetterling, W.T., Flannery, B.P.: In: Numerical Recipes in C, 2nd edn., p.480. Cambridge University Press, New York (1999)
16. Housley, R.M., Grant, R.W., Gonser, U.: Phys. Rev. Lett. **178**, 514 (1969)
17. Jackson, J.D.: In: Classical Electrodynamics, 3rd edn., p.437. Wiley, Hoboken, NJ (1999)
18. Jackson, J.D.: In: Classical Electrodynamics, 3rd edn., p.431. Wiley, Hoboken, NJ (1999)
19. Edmonds, A.R.: In: Angular Momentum in Quantum Mechanics, p.42. Princeton University Press, Princeton, New Jersey (1957)